Flow Turbulence Combust (2016) 96:327–341
DOI 10.1007/s10494-015-9644-y

Multi-Technique Analysis of Soot Reactivity from Conventional and Paraffinic Diesel Fuels

M. Lapuerta[1] · J. Rodríguez-Fernández[1] · J. Sánchez-Valdepeñas[1] · M. S. Salgado[2]

Received: 11 March 2015 / Accepted: 24 August 2015 / Published online: 8 September 2015

Abstract A 2.0 L, 4-cylinder, turbocharged, common rail diesel engine was used for generating soot samples. Three fuels were tested: a "first fill" diesel fuel, a gas-to-liquid fuel (GTL) and a hydrotreated fuel derived from vegetable oils (HVO). A stationary low-load operating mode (1667 rpm and 78 Nm) was selected for testing, and some modifications in the injection process (strategy, timing and pressure) were evaluated experimentally to assess their influence in the soot reactivity. The collected soot samples were characterized using a thermogravimetric analyzer (TGA), a differential scanning calorimeter (DSC), a diffuse reflectance infrared Fourier transform spectrometer (DRIFTS) and a surface area analyzer. All techniques anticipated that HVO and GTL soot samples are more reactive (i.e. show higher potential to be oxidized at lower temperatures leading to more efficient regeneration processes in a Diesel Particle Filter – DPF) compared to diesel soot. Additionally, the four characterization techniques showed the same tendencies when analyzing the effect of the engine operating parameters. In view of the results, the paraffinic fuels – HVO and GTL – here tested confirm their promising perspective for future use in automotive diesel engines, while some guides are proposed to enhance the soot reactivity via calibration of engine operating parameters.

Keywords Soot reactivity · Diesel engine · Paraffinic fuels · Soot analysis techniques

✉ M. Lapuerta
Magin.Lapuerta@uclm.es

[1] Escuela Técnica Superior de Ingenieros Industriales, University of Castilla-La Mancha, Avda. Camilo José Cela s/n, 13071 Ciudad Real, Spain

[2] Physical Chemistry Department, University of Castilla-La Mancha, Avda. Camilo José Cela s/n, 13071 Ciudad Real, Spain

1 Introduction

Transport, and specifically vehicle traffic, has massively increased in the cities in the last decades, standing out as one of the biggest pollutant sources to the atmosphere. Transport emissions have a direct effect in the human health [1, 2] and in the Earth's climate [3–5]. Diesel vehicles share in the passenger car segment has increased across Europe for 35 years (the so-called "dieselization" process), from 10 % in the early 80 s to more than 50 % currently. This figure is even higher in some European nations such as France or Spain. The main pollutants from diesel engines are nitrogen oxides (NOx) and particulate matter (PM).

Within this context users and vehicle manufacturer's concern about environmental problems associated to pollutant emissions has increased. Under the new regulatory laws, vehicle manufacturers have been forced to reduce emissions. Stringent regulations have been published all over the world to reduce transport pollutant emissions.

Light diesel vehicles were committed by Euro 5 Standard [6] to reduce 80 % particulate matter and 20 % nitrogen oxides from Euro 4 Standard. Furthermore, Euro 6 Standard [7], which entered into force in 2014, imposes an additional pollutant decrease. Nitrogen oxides may be reduced drastically by running high EGR ratios [8] at the cost of increasing the particulate matter emissions. Afterwards particulate matter emissions may be collected with a post-treatment system in the exhaust (particulate filter) [9–11]. These particulate filters (DPF) trap the soot (main component of particulate matter), which is latter eliminated in a regeneration process once a sufficient amount of soot has been accumulated.

The aim of this work is to understand the relationship between soot properties (physical, chemical) and its expected behaviour in a DPF regeneration process. This critical process is affected by different factors like i) exhaust gas composition, temperature and flow-rate, ii) filter characteristics and temperature and flow profiles through the filter channels, and iii) physicochemical properties of soot [12–14] which may enhance de oxidation/combustion of soot. The physicochemical properties of soot are the main interest of the present study. The term "reactivity" is used hereinafter to refer to the soot ability to be oxidised at higher rates and/or under a lower temperature environment, which leads to a more efficient regeneration process. In other words, if trapped soot is highly reactive, lower fuel consumption is needed during engine post-injections to reach the soot oxidation temperature.

Another strategy to decrease pollutant emissions in transport is the use of biofuels and alternative fuels [15, 16]. Nowadays, all governments promote the use of biofuels and alternative fuels to replace, at least partially, fossil fuels due to the decrease in oil reserves. For this reason, current directives mandate that renewable energy should share 10 % of the total energy consumption in the transport sector by 2020 [17]. At the present time, the most extended biofuel is biodiesel, used in blends with conventional diesel fuels at a proportion not exceeding (in Europe) 7 %. Distinct alternative fuels emerge as future fuels for the upcoming years. Among these alternatives, paraffinic fuels such as gas-to-liquid (GTL) and hydrotreated vegetable oil (HVO) are already gaining attention. The first one is produced through a Fischer Tropsch process, and among its characteristics stands out the high cetane number and the absence of aromatic compounds. HVO is produced by hydrogenation of a blend of vegetable oils. This fuel possesses very similar physical characteristics to GTL fuel, and may be obtained in current oil refineries.

The reactivity of soot generated from the combustion of different fuels has gained attention recently. Most workers focus on biodiesel. Soot from biodiesel showed (compared to diesel soot) a more amorphous structure [18], a lower temperature for oxidation in a controlled atmosphere [19], smaller primary particles and a higher active surface [12], all

increasing the rate of regeneration of filters, although the magnitude of these benefits seems to depend on the biodiesel origin (longer ester chains exhibit lower oxidative reactivity [20]). Also a lower amount of aliphatic and sulfate-like functionality was reported for biodiesel soot compared to diesel's [21]. There is more dispute around soot coming from Fischer-Tropsch (FT) fuels. Oxidation tests under controlled atmospheres and temperature programs revealed a lower reaction rate for FT soot compared to diesel's and image analyses reported longer fringes (therefore lower amount of edge active sites) for FT soot [22], both suggesting a slower regeneration process in a DPF. However, when tested in a DPF-equipped vehicle no differences were observed between the regeneration process with GTL and normal diesel fueling [23]. Few studies report on the HVO soot characteristics [24], and the preliminary results point out towards a more efficient DPF regeneration compared to diesel.

According to this state of the art, the effect that the novel diesel paraffinic fuels have on the soot properties and thus on the regeneration of after-treatment filters is not confirmed yet. In the present study, soot generated by running a commercial automotive diesel engine with conventional and paraffinic fuels is characterized through different techniques. Soot surface composition, surface area and soot oxidation patterns are presented aiming to assess the ability of the soot to be readily regenerated. As far as we know, this is the first time that the surface area and the surface functionalities of HVO soot are evaluated. The results presented here provide useful information about the compatibility of new alternative fuels and new after-treatment techniques, since both must co-exist in the present and future to comply with the renewable energy and emissions targets.

2 Experimental

2.1 Engine

Soot analyzed in this study was generated in a four cylinder, 4-stroke, turbocharged, intercooled, common-rail, 2.0 L Nissan diesel engine (model M1D), fulfilling Euro 5 Standard. It is originally equipped with intercooled exhaust gas recirculation (EGR), whose temperature is externally controlled, oxidation catalyst (DOC) and regenerative wall-flow type DPF. The engine was coupled to an asynchronous electric brake Schenck Dynas III Li 250. The main specifications of the engine are given in Table 1. In addition, the test engine

Table 1 Diesel engine characteristics

Fuel injection system	DI, common-rail
Cylinders	4
Valves	16
Bore (mm)	84
Stroke (mm)	90
Compression ratio	16:1
Displacement (cm^3)	1994
Maximum power (kW)	111 @ 4000 rpm
Maximun torque (Nm)	323 @ 2000 rpm
Weight (kg)	215

was fitted with the necessary instrumentation for measuring and recording temperature and pressure in different subsystems (intake air, fuel, exhaust gases, lube oil, etc). The INCA PC software and the ETAS ES 591.1 hardware were used for the communication and management of the electronic control unit (ECU). This allows setting engine operating conditions such as injection pressure, injection timing and injection strategy, among other variables.

The exhaust configuration was modified to include a by-pass system (Fig. 1) that enables the user to collect the soot in a stainless steel structure which is previously filled with stainless steel mesh (which acts as a filtering medium). The exhaust gas flows through the mesh where soot is deep trapped, as it is in a flow-through filter, avoiding soot agglomeration. This is different from the trapping process of wall-flow filters, where soot agglomerates forming a soot cake on the porous walls. The structure is then disassembled and the mesh is softly shaken to separate the soot, which is kept for analysis. With this trapping system it is possible to collect a large amount of soot in a reasonable time, which enables performing analyses with a large sample mass requirement (such as the surface area analysis here presented). This is an advantage compared to the traditional trapping method based on pushing a reduced exhaust flow through a filter.

2.2 Fuels

The engine was run with three fuels. A petroleum "first-fill" diesel fuel that meets the EN-590 Standard with no biodiesel content, and was donated by Repsol Corporation (Spain). It is used in cars exported abroad to avoid filter plugging in harsh weather. This fuel was used as a reference fuel for comparison with two alternative paraffinic fuels: a GTL and a HVO fuel. The first one is a gas-to-liquid fuel (GTL) produced through a low temperature Fischer Tropsch process (LTFT) from natural gas, and it was directly donated by Sasol. This type of fuel is almost purely paraffinic, therefore containing nil aromatic content. Finally the HVO fuel was produced by hydrogenation of a blend of oils including palm, camelina and other residual oils. This fuel was donated by Neste Oil Corporation (Finland) and contains lubricity additives. Hydrotreating is one of the most promising biofuel production technologies because of its potential to reduce costs (it can be integrated with current fuel processes in refineries) and to achieve high quality fuels.

The composition and main properties of the fuels are shown in Table 2. The effect of these fuels on the engine emissions and combustion was presented in [25].

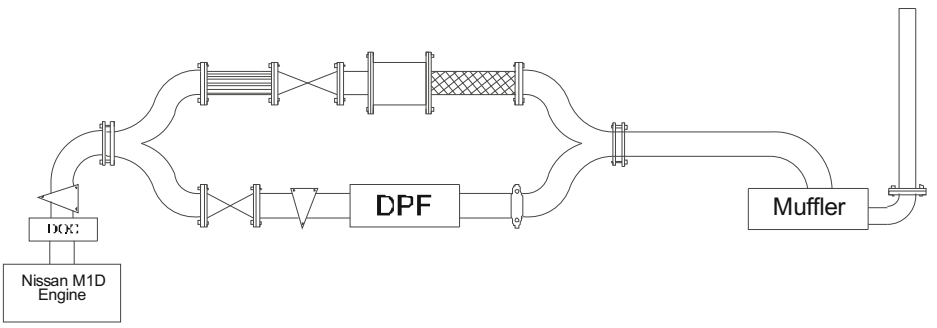

Fig. 1 Configuration of the engine exhaust and bypass system

Table 2 Fuel properties

Properties	Diesel	HVO	GTL
Density at 15 °C (kg/m^3)	811	779.6	774
Viscosity at 40 °C (cSt)	2.015	2.99	2.34
Lubricity (WS1.4, µm)	226	334	211
Lower heating value (MJ/kg)	43.044	43.955	44.03
CFPP (°C)	−30	−21	−7
Ester content (% w/w)	0	0	0
Aromatic content (% w/w)	17.2	0	0
Cetane number	67	94.8	89.2
Acid number	0.16	0.06	0.20
Sulfur (ppm w/w)	< 10	< 10	< 10
Water (ppm w/w)	60	19.2	20
C (% w/w)	85.74	84.68	84.82
H (% w/w)	14.26	14.525	15.18
O (% w/w)	0	0	0
Molecular formula	$C_{13.39}H_{26.72}$	$C_{13.95}H_{28.7}$	$C_{16.89}H_{36.26}$
Molecular weight	187.4	196.1	238.9

2.3 Engine operation mode

Accelerating, decelerating, idle and constant velocity sequences that comprised the New European Driving Cycle (NEDC) that light vehicles must follow in Europe for certification were converted into engine operating modes, defined by torque and engine speed values and thus independent of the properties of the fuel used. The procedure followed was previously published [26]. One operation mode, denoted as U9, was selected from an accelerating sequence of the first sub-cycle; therefore it is an illustrative mode of urban driving conditions. This mode (see specification in Table 3) was selected because it is a low load operation mode characterized by high EGR ratio (which promotes soot formation) and low exhaust temperature (which slows down the spontaneous regeneration of the collected soot). Therefore, this mode is the best mode among those composing the NEDC to represent particulate

Table 3 Characteristics of original U9 mode

Measured variables	Units	U9 Mode
Engine speed	rpm	1667
Effective torque	Nm	78
EGR Ratio	%	22–23
Air flow	kg/h	≈ 78
Start of main injection	°CA (aTDC)	5
Start of pilot injection	°CA (bTDC)	12.7
Fuel injected during pilot injection	µL/inj	1.86
Injection pressure	bar	660

emissions and accumulation in the DPF, and additionally, it accelerates the soot collection rate in the filtering mesh.

Some modifications in the injection settings of the U9 mode were proposed to evaluate their influence in the soot reactivity. Such modifications are indicated in Fig. 2, were injection pressure, injection strategy and injection timing are indicated in three independent axis that meet in a point (the U9 mode). The modifications evaluated were as follows:

- Injection strategy of U9 mode includes a pilot injection followed by the main injection. From this strategy, two variations were evaluated. The first one is a more traditional strategy consisting in a single injection. This strategy allows evaluating the effect of the premixed combustion on soot reactivity, since premixed combustion is enhanced by removing the pilot injection. The second modification added one post injection to the U9 mode (thus working with a pilot, the main and a post injection), in line with current injection trends for reducing engine-out PM emissions and improving the performance of after-treatment techniques. This modification allows determining whether the post injection affects or not soot reactivity.
- Injection pressure of U9 mode is 660 bar; modern injection systems such as the common rail featured by the engine here tested permit a wide range of injection pressures, and the current tendency goes towards higher pressures for improving fuel atomization. Thus, injection pressure was increased up to 720 bar (10 % from the set point of U9 mode) to assess any effect on soot characteristics.
- Main injection for U9 mode starts at 5° CA aTDC, as usual in modern automotive diesel engine for limiting NO_x emissions. Modifications of injection timing consisted in moving the start of injection of the pilot and main events 2° CA back and forward from U9 settings. The injection timing modifies the combustion process and this may affect the soot reactivity.

2.4 Analytical techniques

A TGA (Thermogravimetric Analyzer) from TA Instruments, model Q500, was used to oxidize the soot collected. In this equipment, the sample is located in a crucible inside a small furnace (to reduce the resistance associated with the heat-transfer process), where

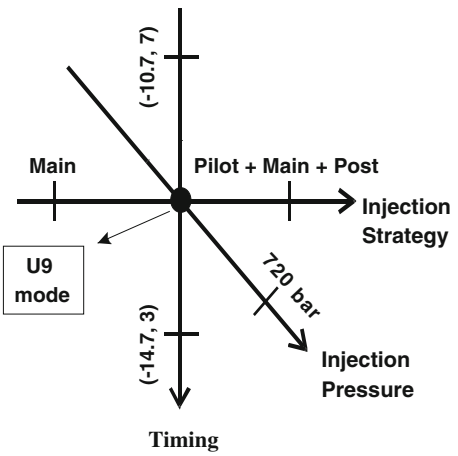

Fig. 2 Modifications in the selected operating mode

the temperature is increased following a user-defined program [27] and the weight loss is continuously recorded. A sample mass of 3 mg was used in all tests. This value was previously selected [27] based on repeatability and reaction regimes issues. The soot sample was heated up to 400 °C under nitrogen atmosphere and maintained at that temperature for an hour to remove the water and volatile organic fraction (pre-treatment period). Then, the sample was cooled down to 100 °C and heated again up to 650 °C with a thermal ramp of 1 °C/min under air atmosphere to complete the oxidation process.

A DSC (Differential Scanning Calorimetry) for TA Instruments, model Q20, was used together with the TGA to complement the results. In this equipment the heat released or absorbed by the sample and its temperature are measured and recorded. When the sample undergoes a physical or chemical transformation involving a heat flow, a temperature difference appears between two capsules (an empty one used as reference and the sample-containing capsule). This temperature difference is related to the heat quantity through an internal calibration. In this equipment the soot sample followed the same oxidation program than the above proposed for the TGA, therefore the results obtained with TGA and DSC are complementary [28–30]. Each sample was measured twice with TGA and DSC, thus the average value is represented in the figures accompanied by a bar with the two ends indicating the lowest and the highest measured values.

DRIFTS (Diffuse reflectance infrared Fourier Transform Spectroscopy) experiments were carried out using an IR-Prestige 21 FTIR spectrometer. DRIFTS is an IR technique used for the study of functional groups adsorbed on soot surface. A Harrick Scientific model DRP-M-05 focuses the IR radiation onto the sample and recollects the dispersed radiation (diffuse reflectance) transporting it to the detector by means of a system of mirrors. The equipment gives as a result the absorbance of the sample analyzed as a function of the wavenumber of the radiation. The low temperature reaction chamber Harrick Scientific model CHC-CHA-3 was installed. The sample was placed in the sample cup, and the cell was closed attaching the dome. Inside this cell, vacuum was done with a pumping system. IR radiation enters and leaves the sample through two ZnSe windows that are located in the dome. Soot samples were previously diluted 1:500 with KBr. The dilution with an inert material allows the IR radiation which reaches the sample to enter deeper into it without being fully absorbed [31, 32]. A previous repeatability study was performed for calculating the standard deviation, which is represented with bars in the graphs.

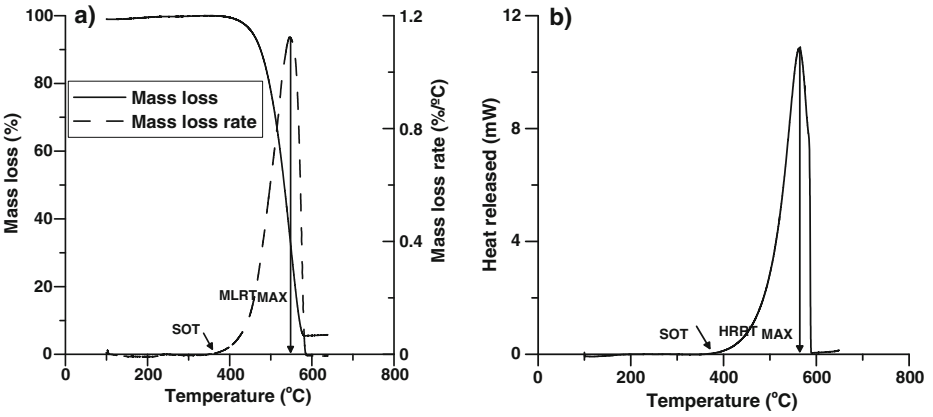

Fig. 3 **a** Typical thermogravimetric soot profile. **b** Typical differential scanning calorimetry profile

Surface area and pore volume were analyzed using a GEMINI V surface area analyzer from Micromeritics Instrument Corporation. Firstly, samples were outgassed for 24 h at 250 °C to remove the moisture and adsorbed compounds. Then the samples were analyzed by the BET [33] nitrogen physisorption method which is used to calculate surface areas [34, 35]. As with DRIFTS equipment, the bars in the graphs indicate the standard deviation calculated in a repeatability study.

3 Results and Discussion

A typical thermogravimetric soot profile is shown in Fig. 3a, where the pre-treatment period (devolatilization under nitrogen atmosphere) is not shown. In the figure, the mass loss and the mass loss rate are presented. Two temperature-based indicators about soot reactivity are the starting oxidation temperature (*SOT*) and the maximum mass loss rate temperature ($MLRT_{MAX}$), both defined and used in previous works [27]. *SOT* represents the temperature during the heating ramp at which the oxidation process starts. With DSC, this temperature cannot be determined accurately due to the decreasing trend of the heat flow at the initial stages, see Fig. 3b (the decreasing trend is a consequence of the endothermic heating of the soot sample). With TGA, this temperature is determined in practice when the mass loss rate surpasses a minimum threshold, established in 0.01 %/°C. $MLRT_{MAX}$ represents the temperature when soot reaches the maximum mass loss rate in the TGA. The equivalent indicator in the DSC is the maximum heat release rate temperature ($HRRT_{MAX}$), representing the temperature when the heat release rate during the soot oxidation is maximum.

Figures 4 and 5 show the evaluation of the soot samples in the TGA and the DSC, respectively, and following the experimental matrix shown in Fig. 2. In the case of TGA, two tests were carried out for each sample since the repeatability is lower than that of DSC (due to the bigger size of the furnace and because the thermocouple is not directly in contact with the sample) and error bars are included.

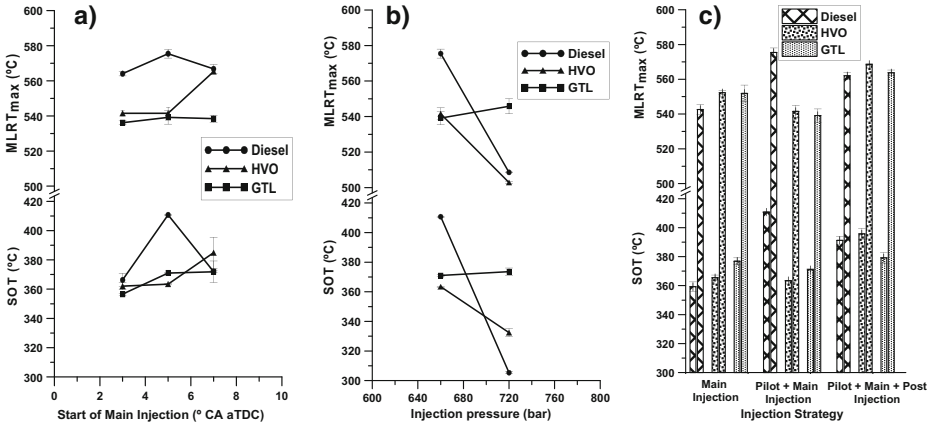

Fig. 4 **a** SOT and $MLRT_{MAX}$ trend with start of main injection. **b** SOT and $MLRT_{MAX}$ trend with injection pressure. **c** SOT and $MLRT_{MAX}$ trend with injection strategy

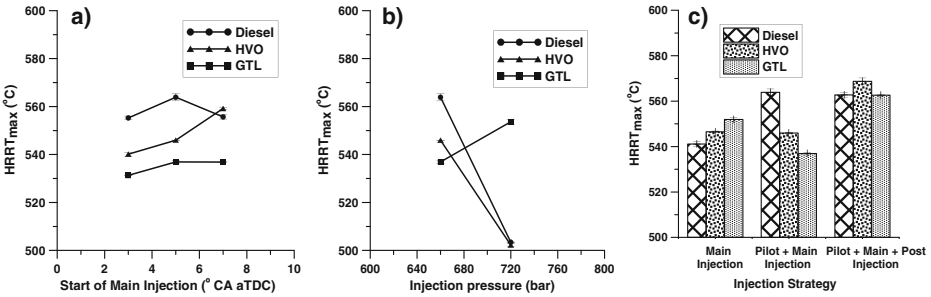

Fig. 5 **a** $HRRT_{MAX}$ trend with start of main injection. **b** $HRRT_{MAX}$ trend with injection pressure. **c** $HRRT_{MAX}$ trend with injection strategy

As can be seen in Figs. 4 and 5 similar trends for $MLRT_{MAX}$ and $HRRT_{MAX}$ were obtained with TGA and DSC (higher temperature indicates lower reactivity). In Figs. 4a and 5a when start of main injection is advanced 2° CA from the cartography setpoint the reactivity of the soot samples increases. Less conclusive is the effect of delaying the injection, since there is not an obvious trend because reactivity increases for diesel soot, decreases for HVO soot and shows no change for GTL soot. It seems clear that when the engine was running with diesel the soot reactivity was lower that when it was running with HVO and GTL. Among the alternative fuels tested, the results reveal that GTL soot is more reactive than HVO soot. By increasing the injection pressure (Figs. 4b and 5b) a much higher reactivity for diesel and HVO soot is obtained but this trend isn't confirmed with GTL soot. Figures 4c and 5c illustrate the effect of the injection strategy in soot reactivity. When a pilot injection is added to the main injection an increase in the reactivity is observed for HVO and GTL soot, but this trend is not replicated by diesel soot. If a post injection is added to the injection strategy a reactivity increase takes place with diesel soot, but again the opposite trend is observed with HVO and GTL soots. Furthermore, similar trends were observed for SOT and $MLRT_{MAX}$ in the TGA results, therefore both temperatures may be used when discussing the reactivity of different soot samples.

Figure 6 shows the results obtained with the surface area and pore size analyzer. It may be hypothesized that as the surface area increases the oxygen has a better access to the carbonaceous substrate, thus the soot reactivity is enhanced. As illustrated, the three

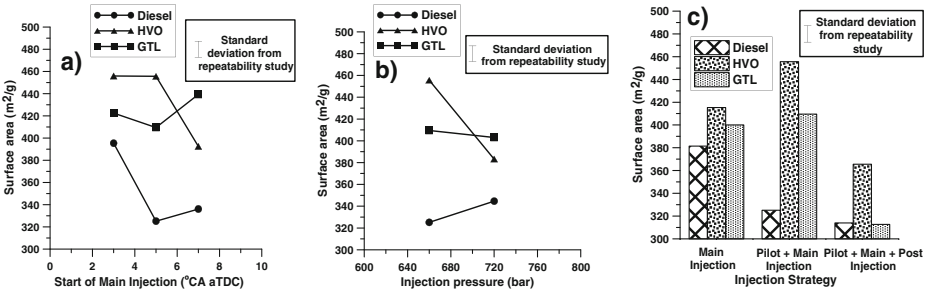

Fig. 6 **a** Surface area trend with start of main injection. **b** Surface area trend with injection pressure. **c** Surface area trend with injection strategy

fuels follow in general the same trend described for TGA and DSC when the start of main injection, the injection pressure or the injection strategy were changed. As a rule, it can be seen that diesel soot is less reactive than HVO and GTL soot, and this trend agrees with the obtained from TGA and DSC as well. However, Fig. 6a and c show a higher surface area for HVO soot than for GTL soot and therefore the first one is anticipated to have higher reactivity but this trend isn't consistent with TGA and DSC results. In respect to the effect of the injection pressure, Fig. 6b shows that the reactivity of diesel soot increases and reactivity of GTL soot marginally decreases with injection pressure, in line with TGA/DSC results. However, in the case of HVO soot its reactivity decreases with the injection pressure, being this opposite to the trend obtained with TGA/DSC.

Figure 7 shows a typical spectrum obtained when soot is analyzed with DRIFTS (only one spectrum is represented to avoid too many traces, since the other soots from different fuels and injection settings present the same bands in the spectrum). In that spectrum different bands are observed and their assignment to functional groups is presented in Table 4.

Figures 8 and 9 show the concentration of hydroxyl and carbonyl/carboxylic functional groups, respectively, for diesel, HVO and GTL soots, for all the injection settings tested. This concentration can be considered proportional to the area under the 3500–3100 cm^{-1} band and under 1730–1660 cm^{-1}. These areas have been calculated solving the corresponding integral.

According to the repeatability study previously carried out (see error bars in figures) no significant differences are observed for many of the strategies selected. Nevertheless, the trends obtained in Figs. 8 and 9a, b and c are similar than those obtained with TGA, DSC and surface area and pore size analyzer.

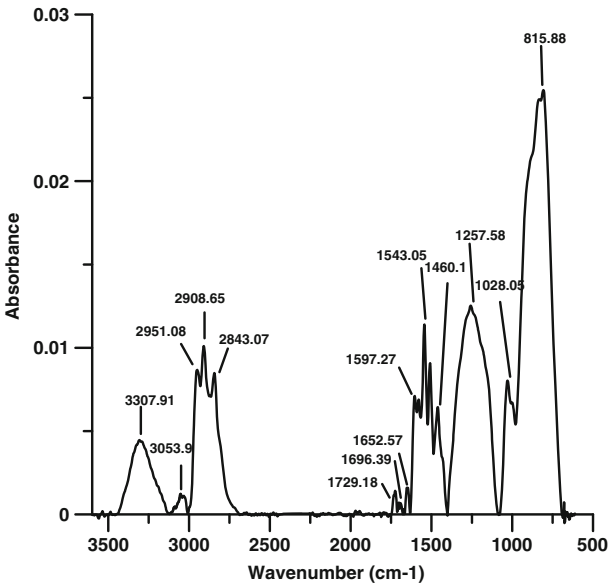

Fig. 7 Typical soot spectrum obtained with DRIFTS. This spectrum corresponds to Diesel fuel and mode U9

Table 4 Assignment of infrared absorption peaks to functional groups

Wavenumber (cm^{-1})	Assignments	Literature reports
3500 – 3100	O-H stretch in hydroxyl groups	[36–38]
3050	Aromatic C-H stretch	[36, 38–42]
2960	Asymmetric CH_3 stretch	[36, 43]
2920	Asymmetric CH_2 stretch	[36, 43]
2850	Symmetric CH_3 stretch	[40, 41]
1772–1660	Alkenes C=C stretch	[44]
	C=O stretch in carbonyl groups	[42, 43]
1729	C=O stretch in carboxylic groups	[36, 39, 40, 45]
1669–1513	CΞC	[42, 43, 46]
1600–1460	C=O stretch in carboxylic groups	[47]
	C=C	[45, 48]
1600	Aromatic C=C enhanced by C=O conjugation	[36, 40]
1595	Aromatic and alkene C=C stretch	[39, 41]
1460	= CH_2 stretch	[36, 37, 40, 42]
1400–1100	C-C and C-H plane deformation of aromatic groups and ether C-O-C stretching	[36, 39, 41]
1100	C-O stretch in ethers, esters, alcohol and phenol	[40]
1050	C-O stretch in hydroxyl groups	[40]
1033	C-O stretch in ether and hydroxyl groups	[42]
1000–750	Aromatic C-H bend	[49]

In respect to fuels, the DRIFTS study shows that, in three of the six mode variations tested (U9, advanced injection and post-injection addition), HVO soot presents more concentration of oxygenated hydroxyl groups than diesel and GTL fuels, and these differences are significant when compared to the width of the error bars. Contrarily, the concentration of carbonyl groups is lower for HVO, but differences are smaller and within the error bars. Nevertheless, it is important to realize that hydroxyl group concentration is higher than that of carbonyl and carboxylic groups, which is consistent with the results

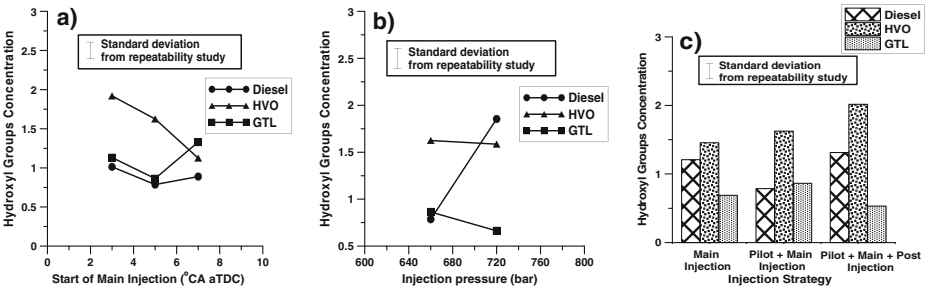

Fig. 8 **a** Trend of hydroxyl groups concentration with start of main injection. **b** Trend of hydroxyl groups concentration with injection pressure. **c** Trend of hydroxyl groups concentration with injection strategy

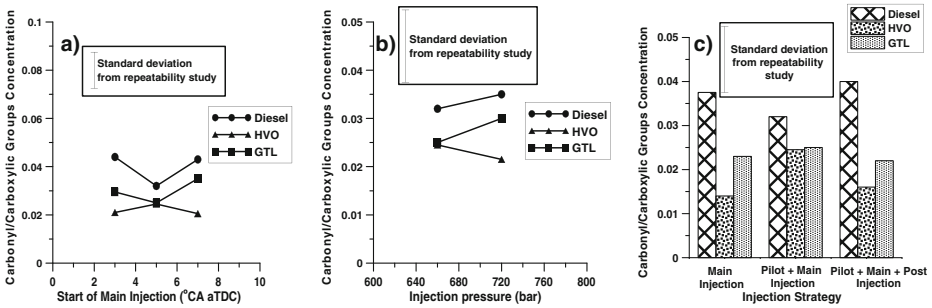

Fig. 9 **a** Trend of carbonyl/carboxylic group concentration with start of main injection. **b** Trend of carbonyl/carboxylic group concentration with injection pressure. **c** Trend of carbonyl/carboxylic group concentration with injection strategy

reported in [50]. This suggests that the high reactivity of HVO soot found with the former techniques may be related to the presence of hydroxyl groups on the soot surface. The consistent results obtained from DRIFTS are encouraging because previous studies performed with x-ray photoelectron spectroscopy did not achieve any clear conclusion about the effect of the fuel on the concentration of oxygen-containing functional groups in the soot [22].

4 Conclusions

A commercial diesel engine compliant with Euro 5 emission Standard and equipped with a regenerative wall-flow type DPF was tested with three different fuels and under several injection strategies, selected to evaluate their impact in soot reactivity. The results obtained with thermogravimetric analyzer, differential scanning calorimetry, surface area and pore size analyzer and DRIFTS show the same general trends between injection settings. As a rule, advancing 2° CA the start of injection decreases the soot samples reactivity, but the effect of delaying the injection is less evident. Increasing the injection pressure improves the reactivity of diesel soot but worsen the GTL soot reactivity (no conclusion may be obtained about HVO soot since different techniques point out different trends). If the engine is fuelled with paraffinic fuels, removing the pilot injection or adding a post injection leads to a more reactive soot.

Regarding the effect of the fuel, results with TGA, DSC and surface area analyzer confirm that soot obtained from diesel fuel is less reactive than HVO and GTL soot. The identification of chemical groups performed with DRIFTS shows that HVO soot has higher concentration of oxygenated hydroxyl groups. Oxygen availability on the soot surface is expected to increase the soot reactivity.

Both alternative fuels showed a good potential for future use in diesel engines. Despite other advantages well documented in literature (related to emissions), this work confirms that such fuels reduce the temperature required for soot oxidation, leading to more efficient regeneration processes and lower fuel consumption.

Finally, the combination of different chemical and structural techniques has been proved to be essential for a consistent qualitative determination of the reactivity of soot from different fuels and under different injection settings.

Acknowledgments This study has been carried out under the framework of project ENE2013-48602-C3-1-R, financed by the Spanish Ministry of Economy and Competitiveness. The authors also wish to acknowledge to the companies Repsol, (Spain), Sasol (South Africa) and Neste Oil (Finland), for supplying the fuels tested, and Nissan Motor Ibérica (Spain), for the donation of the engine tested.

References

1. Dockery, D.W., Schwartz, J., Spengler, J.D.: Air pollution and daily mortality: associations with particulates and acid aerosols. Environ. Res. **59**, 362–373 (1992)
2. Pourazar, J., Frew, A.J., Blomberg, A., Helleday, R., Kelly, F.J., Wilson, S.: Diesel exhaust exposure enhances the expression of IL-13 in the bronchial epithelium of healthy subjects. Respir. Med. **98**, 821–825 (2004)
3. Goyal, P., Jaiswal, N., Kumar, A., Dadoo, J.K., Dwarakanath, M.: Air quality impact assessment of NO_x and PM due to diesel vehicles in Delhi. Transport Res. Transport Environ. **15**, 298–303 (2010)
4. Jacobson, M.Z.: Global direct radiative forcing due to multicomponent antrophogenic and naturals aerosols. J. Geophys. Res. **106**, 1551–1568 (2001)
5. Koch, D.: Transport and direct radiative forcing of carbonaceous and sulphate aerosols in the GSISS GCM. J. Geophys. Res. **106**, 20311–20332 (2001)
6. Directive 715/2007/CE of the European Parliament and of the Council (2007)
7. Directive 136/2014/CE of the European Parliament and of the Council (2014)
8. Abu-Jrai, A., Rodríguez-Fernández, J., Tsolakis, A., Megaritis, A., Theinnoi, K., Cracknell, R.F.: Performance, combustion and emissions of a diesel engine operated with reformed EGR. Comparison of diesel and GTL fuelling. Fuel **88**, 1031–1041 (2009)
9. Johnson, J.H., Bagley, S.T., Gratz, L.D., Leddy, D.G.: A review of diesel particulate control technology and emissions effects – 1992 Horning Memorial Award Lecture. SAE International Congress and Exposition (1992)
10. Neeft, J.P.A., Makkee, M., Moulijn, J.A.: Diesel particulate emissions control. Fuel Process. Tech. **47**, 1–69 (1996)
11. Eastwood, P.: Critical topics in exhaust gas aftertreatment. Research Studies Press, Baldock, Hertfordshire (2000)
12. Lapuerta, M., Oliva, F., Agudelo, J.R., Boehman, A.L.: Effect of fuel on the soot nanostructure and consequences on loading and regeneration of diesel particulate filters. Combust. Flame **159**, 844–853 (2012)
13. Vander Wal, R.L., Tomasek, A.J.: Soot oxidation: dependence upon initial nanostructure. Combust. Flame **134**, 1–9 (2003)
14. Vander Wal, R.L., Tomasek, A.J.: Soot oxidation: dependence upon synthesis conditions. Combust. Flame **136**, 129–140 (2004)
15. Lapuerta, M., Armas, O., Rodríguez-Fernández, J.: Effect of biodiesel fuel son diesel engine emissions. Prog. Energy Combust. Sci. **34**, 198–223 (2008)
16. Gill, S.S., Tsolakis, A., Dearn, K.D., Rodríguez-Fernández, J.: Combustion characteristics and emissions of Fischer-Tropsch diesel fuels in IC engines. Prog. Energy Combust. Sci. **37**, 503–523 (2011)
17. Directive 28/2009/CE of the European Parliament and of the Council (2009)
18. Boehman, A.L., Song, J., Alam, M.: Impact of biodiesel blending on diesel soot and the regeneration of particulate filters. Energ Fuel **19**, 1857–1864 (2005)
19. Williams, A., Black, S., McCormick, R.L.: Biodiesel fuel property effects on particulate matter reactivity. In: 6th International Exhaust Gas and Particulate Emission Forum, Ludwigsburg, Germany, March 9–10. Available in http://www.gulfhydrocarbon.com/forms/BiodieselFuelProperty%20EffectsonParticulateMatterReactivity.pdf (2010). Accessed 31 Aug 2015
20. Barrientos, E., Maricq, M., Boehman, A., Anderson, J.: Impact of Ester Structures on the Soot Characteristics and Soot Oxidative Reactivity of Biodiesel. SAE Technical Paper 2015-01-1080 (2015). doi:10.4271/2015-01-1080
21. Salamanca, M., Mondragón, F., Agudelo, J.R., Santamaría, A.: Influence of palm oil biodiesel on the chemical and morphological characteristics of particulate matter emitted by a diesel engine. Atmosph. Env. **62**, 220–227 (2012)
22. Yehliu, K., Vander Wal, R.L., Armas, O., Boehman, A.L.: Impact of fuel formulation on the nanostructure and reactivity of diesel soot. Combust. Flame **159**, 3597–3606 (2012)

23. Liebig, D., Clark, R., Muth, J., Drescher, I.: Benefits of GTL Fuel in Vehicles Equipped with Diesel Particulate Filters. SAE Technical Paper 2009-01-1934 (2009). doi:10.4271/2009-01-1934
24. Bhardwaj, O.P., Lüers, B., Holderbaum, B., Koerfer, T., Pischinger, S., Honkanen, M.: Utilization of HVO fuel properties in a High Efficiency Combustion System: Part 2: Relationship of Soot Characteristics with its Oxidation Behavior in DPF. SAE Technical Paper 2014-01-2846 (2014). doi:10.4271/2014-01-2846
25. Armas, O., García-Contreras, R., Ramos, A., López, A.F.: Impact of animal fat biodiesel, GTL, and HVO fuels on combustion, performance, and pollutant emissions of a light-duty diesel vehicle tested under the NEDC. J. Energy Eng. **141**(2), C4014009 (2015)
26. Lapuerta, A., Hernández, J.J., Giménez, F.: Evaluation of exhaust gas recirculation as a technique for reducing diesel engine NOx emissions. Proc. Instn. Mech. Engrs. D **214**, 85–93 (2000)
27. Rodríguez-Fernández, J., Oliva, F., Vázquez, R.: Characterization of the diesel soot oxidation process through an optimized thermogravimetric method. Energ Fuel **25**, 2039–2048 (2011)
28. Song, J., Alam, M., Boehman, A.L.: Impact of alternative fuels on soot properties and DPF regeneration. Combust. Sci. Tech. **179**, 1991–2037 (2007)
29. Williams, A., McCormick, R.L., Hayes, R., Ireland, J., Fang, H.L.: Effect of biodiesel blends on diesel particulate filter performance. SAE Technical Paper 2006-01-3280 (2006)
30. Stratakis, G.A., Stamatelos, A.M.: Thermogravimetric analysis of soot emitted by a modern diesel engine run on catalyst-doped fuel. Combust. Flame **132**, 157–169 (2003)
31. Muckenhuber, H., Grothe, H.: A DRIFTS study of the heterogeneous reaction fo NO_2 with carbonaceous materials at elevated temperature. Carbon **45**, 321–329 (2007)
32. Hernández-Giménez, A.M., Lozano-Castelló, C., Bueno-López, A.: Effect of CO_2, H_2O and SO_2 in the ceria-catalyzed combustión of soot under simulated diesel exhaust conditions. Appl. Catal. B Environ. **148–149**, 406–414 (2014)
33. Brunauer, S., Emmett, P.H., Teller, E.: Adsorption of gases in multimolecular layers. J. Am. Chem. Soc. **60**, 309–319 (1938)
34. Fernandes, M.B., Skjemstad, J.O., Johnson, B.B., Wells, J.D., Brooks, P.: Characterization of carbonaceous combustion residues. I. Morphological, elemental and spectroscopic features. Chemosphere **51**, 785–795 (2003)
35. Tighe, C.J., Twigg, M.V., Hayhurst, A.N., Dennis, J.S.: The kinetics of oxidation of Diesel soots by NO_2. Combust. Flame **159**, 77–90 (2012)
36. Russo, C., Stanzione, F., Tegrossi, A., Alfè, M., Ciajolo, A.: The effect of temperature on the condensed phases formed in fuel-rich premixed benzene flames. Combust. Flame **159**, 2233–2242 (2012)
37. Sánchez Escribano, V., Fernández López, E., Gallardo Amores, J.M., del Hoyo Martínez, C., Pistarino, C., Panizza, M., Resini, C., Busca, G.: Combust. Flame **153**, 97–104 (2008)
38. Hu, S., Xiang, J., Sun, L., Xu, M., Qiu, J., Fu, P.: Characterization of char from rapid pyrolisis of rice husk. Fuel Process. Technol. **89**, 1096–1105 (2008)
39. Santamaría, A., Mondragón, F., Molina, A., Marsh, N.D., Eddigns, E.G., Sarofim, A., F.: FT-IR and ^{1}H NMR characterization of the products of an ethylene inverse diffusion flame. Combust. Flame **146**, 52–62 (2006)
40. Jeremy, P., Gassman, P.L., Wang, H., Laskin, A.: Micro-FTIR study of soot chemical composition-evidence of aliphatic hydrocarbons on nascent soot surfaces. Phys. Chem. Chem. Phys. **12**, 5206–5218 (2010)
41. Santamaría, A., Yang, N., Eddigngs, E., Mondragón, F.: Chemical and morphological characterization of soot and soot precursors generated in an inverse diffusion flame with aromatic and aliphatic fuels. Combust. Flame **157**, 33–42 (2010)
42. Sharma, R., Wooten, J., Baliga, V., Lin, X., Chan, W., Hajaligol, M.: Characterization of chars form pyrolysis of lignin. Fuel **83**, 1469–1482 (2004)
43. Sharma, R., Wooten, J., Baliga, V., Hajaligol, M.: Characterization of chars from biomass-derived materials: pectin chars. Fuel **80**, 1825–1836 (2001)
44. Daly, H.M., Horn, A.B.: Heterogeneous chemistry of toluene, kerosene and diesel soots. Phys. Chem. Chem. Phys. **11**, 1069–1076 (2009)
45. Min, F., Zhang, M., Zhang, Y., Cao, Y., Pan, W.P.: An experimental investigation into the gasification reactivity and structure of agricultural waste chars. J. Anal. Appl. Pyrol. **92**, 250–257 (2011)
46. Uzun, B., Apaydin-Varol, E., Ates, F., Özbay, N., Pütün, A.A.: synthetic fuel production from tea waste. Characterization of bio-oil and bio-char. Fuel **89**, 176–194 (2010)

47. Liu, Z., Zhang, F., Wu, J.: Characterization and application of chars produced from pinewood pyrolysis and hydrothermal treatment. Fuel **89**, 510–514 (2010)
48. Jindaron, C., Meeyoo, V., Kitiyanan, B., Rirksomboon, T., Rangsunvigit, P.: Surface characterization and dye adsorptive capacities of char obtained from pyrolysis/gasification of sewage sludge. Chem. Eng. J. **133**, 239–246 (2007)
49. Molina, A., Mondragón, F.: Reactivity of coal gasification with steam and CO_2. Fuel **77**, 1831–1839 (1998)
50. Wang, L., Song, C., Song, J., Lv, L., Pang, H., Zhang, W.: Aliphatic C-H and oxygenated surface functional groups of diesel in-cylinder soot: characterizations and impact on soot oxidation behaviour. Proc. Comb. Inst. **34**, 3099–3106 (2013)